Time-Lapse Seismic Monitoring of Enhanced Oil Recovery CO_2-Flood in a Thin Carbonate Reservoir, Hall-Gurney Field, Kansas, U.S.A.

Abdelmoneam E. Raef, Richard D. Miller, Alan P. Byrnes, William E. Harrison, and Evan K. Franseen
Kansas Geological Survey, University of Kansas, 1930 Constant Avenue, Lawrence, Kansas 66047-3726

Poster presented at the annual meeting of the American Association of Petroleum Geologists
Calgary, Alberta, Canada, June 22, 2005

Original posters were 32” x 44”
Content was reformatted to 8½ x 11, only layout modified

Open-file Report 2005-24

Time-Lapse Seismic Monitoring of Enhanced Oil Recovery CO_2-Flood in a Thin Carbonate Reservoir, Hall-Gurney Field, Kansas, U.S.A.

Abdelmoneam E. Raef, Richard D. Miller, Alan P. Byrnes, William E. Harrison, and Evan K. Franseen
Kansas Geological Survey, University of Kansas, 1930 Constant Avenue, Lawrence, Kansas 66047-3726

Summary

Efficiency of enhanced oil recovery (EOR) programs relies heavily on accurate reservoir models. Movement of miscible carbon dioxide (CO_2) injected into a thin (~5 m), shallow-shelf, oomoldic carbonate reservoir around 900 m deep in Russell County, Kansas, was successfully monitored using high-resolution 4D/time-lapse seismic techniques. High-resolution seismic methods showed great potential for incorporation into CO_2-flood management, highlighting the necessity of frequently updated reservoir-simulation models, especially for carbonates. Use of an unconventional approach to acquisition and interpretation of the high-resolution time-lapse/4D seismic data was key to the success of this monitoring project.

Weak-anomaly enhancement of selected non-inversion, 4D-seismic attribute data represented a significant interpretation development and proved key to seismic monitoring of CO_2 movement. Also noteworthy was the improved definition of heterogeneities affecting the expanding flood bank. Among other findings, this time-lapse seismic feasibility study demonstrated that miscible CO_2 injected into a shallow, thin carbonate reservoir could be monitored, even below the classic temporal seismic resolution limits.

Objectives: Questions to be Answered

Flood Management

Where is the injected CO_2 going?
What is the sweep efficiency?
Are there any areas of bypassed oil?
How can the injection and production program be improved in near real time to optimize the sweep or recovery?

CO_2 Sequestration

Where is CO_2 moving?
Is it moving outside the pattern?
If CO_2 is moving, what is the mechanism?
How does CO_2 in the reservoir change with time?
Can high-resolution seismic reflection provide the assurances necessary to accurately monitor CO_2 distribution?

Setting the Stage

Time-lapse seismic monitoring of EOR programs in carbonates has seen limited success. This has been due to various non-seismic factors such as:

- highly heterogeneous nature of carbonates,
- diagenetic complications of porosity distribution,
- shallow depth and thinness of many carbonate reservoirs, and
- low compressibilities that reduce fluid-effects.

Other complications related to seismic imaging include:

- resolution limitations,
- low signal-to-noise ratios,
- low-fold coverage at shallow depths, and
- near-surface irregularities.

For 4D-seismic monitoring to successfully provide information necessary for "geosteering" of an EOR program, key factors that must be considered include:

- timeliness,
- repeatability,
- correlation to reservoir properties,
- minimized acquisition times/duration, and
- consistency in seismic attributes.

Carbonate reservoirs represent some of the most significant challenges in seismic imaging and interpretation, but also hold some of the greatest potential for resource development in the midcontinent.

CO_2 EOR Pilot Study

Development of EOR techniques are critical to the eventual recovery of oil bypassed or stranded after water flooding in a large number of Class II reservoirs in the midcontinent. As part of a "Class II Revisit" program funded by DOE, a 10+-acre EOR pilot study was designed to demonstrate the technical feasibility and economic viability of miscible CO_2 flood in a representative Lansing-Kansas City oomoldic limestone shallow-shelf carbonate reservoir. This pilot study involves two production wells, two water injectors, and one CO_2 injector (Figure 1A). Pre-flood reservoir simulation models predict slightly enhanced sweep to the #12 and #13 wells. Since the flood containment is influenced and, to some degree, controlled by injection rates in the #10 and #18 wells, if unplanned movement can be imaged in a timely fashion, predictive simulations can be updated, allowing sweep irregularities and inefficiencies to be controlled by altering injection and production rates.

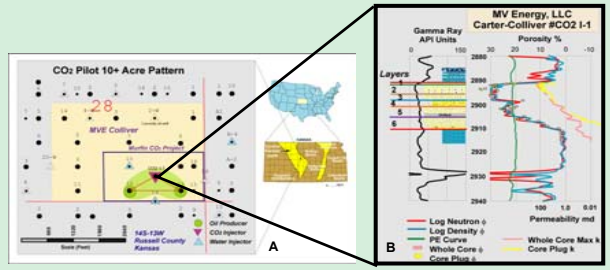

Figure 1. Site map and "C" zone.

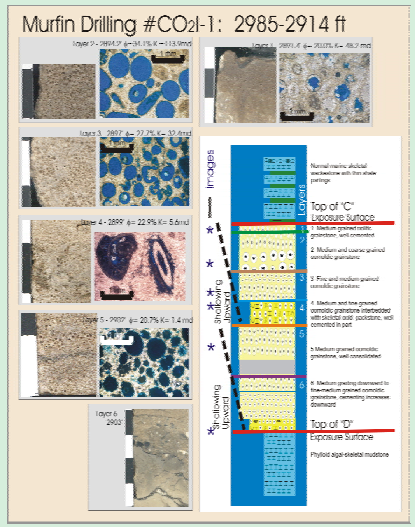

Figure 2. "C" zone geologic description.

The target of this EOR-CO_2 miscible flood is a thin, oomoldic carbonate formation (Plattsburg) "C zone" of the Lansing-Kansas City Group (Figure 1B) in central Kansas, deposited on a shallow marine shelf as part of a sequence of Upper Pennsylvanian depositional cyclothems. Reservoir rocks were deposited as fine-medium-grained ooid sands in shallowing-upward fourth-order sequences (Figure 2). Cyclic carbonate strata of the Pennsylvanian Lansing-Kansas City Group represent important enhanced oil recovery targets on the Central Kansas uplift and thus require understanding of controls on reservoir properties and architecture (Figure 3).

Reservoir Characteristics

Reservoir rocks in the C zone are oolitic grainstones that were originally deposited as shallow marine coarse-grained ooid sands concentrated on bathymetric highs on the shelf. Subaerial exposure and meteoric water percolation in the shallow shelf setting commonly caused ooid dissolution, resulting in oomoldic grainstone textures. The dissolution of ooids along with fracturing and crushing (providing connectivity between ooid molds) resulted in the oomoldic grainstones being the principal reservoir rock type (lithofacies). Each of the stacked cyclic deposits within the C zone is characterized by vertically increasing porosity and permeability resulting in vertical heterogeneity. Previous study of well log and core data indicate lateral lithofacies changes resulting in lateral heterogeneity.

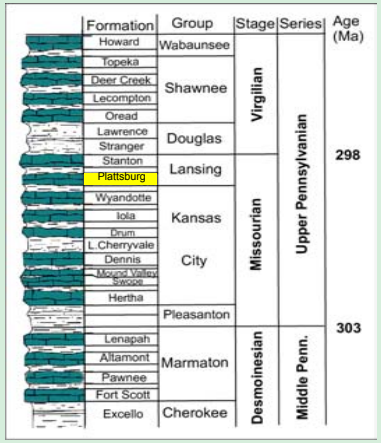

Figure 3. Stratigraphic column for reservoir.

3D Seismic-Reflection Program

Design of the seismic survey focused on optimizing the repeatability, acquisition speed, minimized footprint, and azimuthal and fold coverage, and subsurface resolution. High-fold coverage encompasses an area about five times larger than the anticipated size of the pilot study and planned movement of CO_2 (Figure 4). This enlarged high-fold footprint ensured the expected 400 m^2 flood area was fully sampled. Considering the range of offsets necessary to capture the ideal reflected seismic energy, a source footprint over 1.5 km^2 and receiver spread of 1 km^2 was necessary.

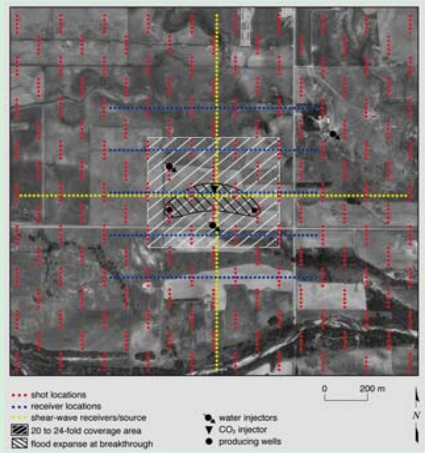

Figure 4. Acquisition geometry.

A modified brick acquisition pattern was selected to optimize azimuthal and offset distributions (Figure 4). This configuration is more difficult to acquire, but provides much better overall bin-level trace properties. A total of 240 receivers were deployed along five lines, each line separated by 200 m and oriented east/west. Source lines were north/south and staggered along lines separated by 100 m. Source station intervals were 20 m, which yielded 10 m x 10 m bins with 20- to 24-fold sampling redundancy within the high-fold coverage area.

A variety of surface obstacles affected data quality and provided challenges during acquisition (Figure 5). Survey repeatability was continuously challenged by a variety of logistical as well as practical problems. A total of nine landowners were affected by the 2.25 km^2 source footprint while geographically within this small area were dozens of pumping units, pastures, cultivated fields, oil field operator storage yards, a major Kansas river, wooded areas, and two county roads.


Figure 5. Pictures from around site.

Considering the need/necessity for repeatability and quiet operations, a high-resolution guidance and surveying system was customized to provide source operators with a real-time digital map and location logging capabilities (Figure 6). Avoiding equalization techniques during data processing as much as possible was deemed essential, considering the required signal-to-noise levels and extreme resolution necessary to detect the CO_2. An overall accuracy of ±5 cm for all x, y, and z source and receiver location measurements was maintained (Figure 7). Each source location was reoccupied during each monitoring survey within a tolerance not exceeding 0.5 m.


Figure 6. GPS on vib.


Figure 7. GPS base station at CO_2 injector.


Figure 8. Vib track.

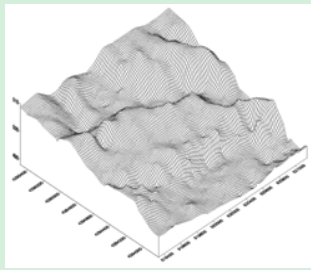
Figure 9. Digital terrain map.

Considering the obstacles around this site, night operations would not have been possible without a pre-mapped route and digital GPS guidance system, with predesigned routes updated continuously through GPS feeds inside the vibrator seismic source (Figure 8). The resulting digital terrain map was incorporated into data processing, providing excellent information for datum corrections (Figure 9).

Data Acquisition

Minimal-channel recording equipment and a single vibratory source were the centerpieces of the acquisition program. Key to this equipment is the low-cost seismic monitoring, small footprint, low maintenance, and dependability.

A 240-channel distributed seismic recording system from Geometrics provided 24-bit A/D, short sampling rates (by conventional standards), and extreme flexibility and durability (Figure 10). Each distributed unit was connected to a set of 24 geophones via analog seismic cable and to a seismic controller by ruggedized Ethernet cables. Data from the ten distributed seismographs (Geodes) were monitored and stored on a specialized land controller also from Geometrics (Figure 11). The controller was housed in a John Deere Gator with a customized all-weather shelter, allowing operations in rain or shine from –40 to over +40° C.


Figure 10. Geode seismographs.


Figure 11. Recording vehicle.


Figure 12. Compressional wave.


Figure 13. Shear wave.

A single IVI minivib II 14,000-lb seismic vibrator with a prototype high-output Atlas rotary-style servo valve provided the seismic energy for these surveys (Figure 12). In-field rotation of the mass allowed either compressional- or shear-wave data to be collected using the same model vibratory source. Compressional-wave energy requires the mass to move in a vertical direction, perpendicular to the ground surface (Figure 12), while for shear-wave energy the motion of the mass was parallel to the ground (Figure 13). Five 10-second upsweeps from 20 to 250 Hz were recorded at each station for compressional waves and five 10-second upsweeps from 10 to 80 Hz for shear waves. The first sweeps were designed to seat the plate only and were not included in processed data.

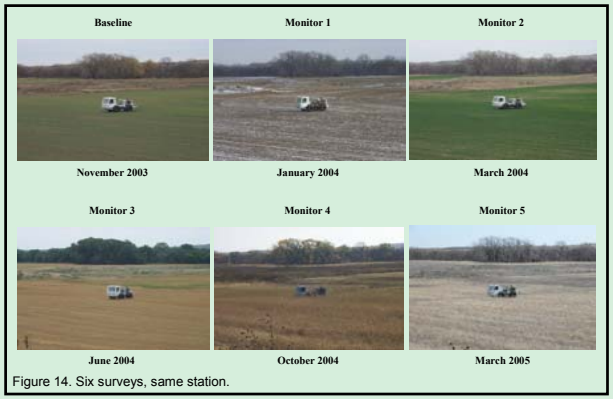

Figure 14. Six surveys, same station.

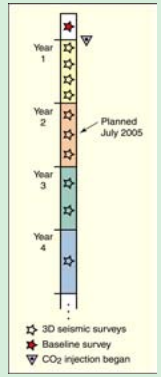

Figure 15. Timeline.

To date, a total of six 3D surveys have been acquired (Figure 14). Time between surveys has gradually increased from six weeks to the current six months between consecutive 3D surveys (Figure 15). Data changes have been observed due to seasonal weather and soil moisture variability. A total of twelve surveys will be necessary to adequately characterize the efficiency and stability of the CO_2 flood and eventual sequestration.

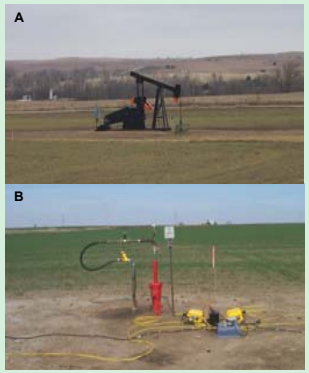

Figure 16. Production well #12 (A), injector #18 (B).

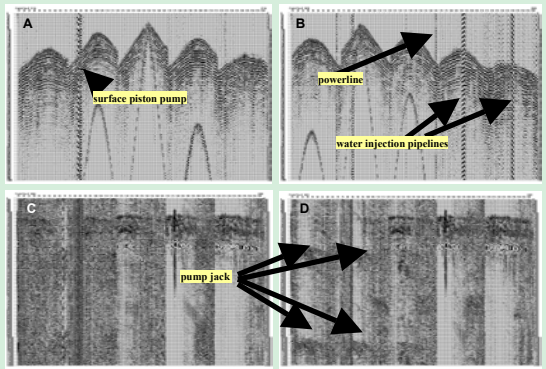

Figure 17. Noise from field activities on seismograms.

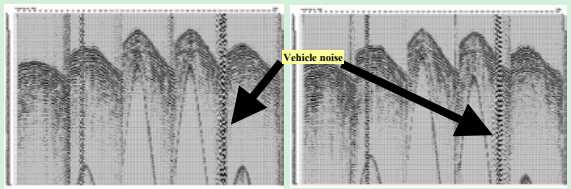

Figure 18. Vehicle noise on seismograms.

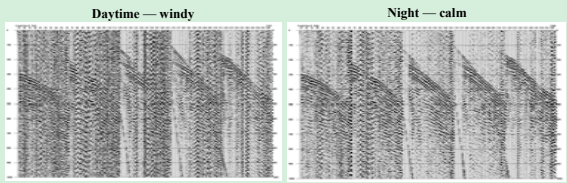

Figure 19. Comparison of wind (20 mph) and calm.

Acquisition Noise

Time-lapse seismic data possess reasonable potential to detect changes in reservoir fluids when all noise—both source and environment—is consistent and minimal. Noise associated with wind, vehicles, transmission lines, and fixed pumping facilities (especially in active oil fields) is a persistent problem with any seismic survey. In an active oil field, production wells (Figure 16A), injection wells (Figure 16B), and flowing pipelines produce noise at saturation levels for most seismic recording systems (Figure 17).

Much of the seismic data were acquired at night to minimize environmental and cultural noise. Vehicle traffic was also greatest during the day. Re-shooting stations when vehicles were within the survey area was generally necessary (Figure 18). Wind was a dominant source of noise during daylight hours (Figure 19). With the very weak anomalies, low signal-to-noise, and high-resolution requirements associated with these kinds of thin, midcontinent carbonate reservoirs, extraordinary care must be taken with respect to minimizing noise.

Basic Data Processing

With the need for horizon-based interpretations and a high-resolution image of the CO_2 plume as it expands across the site, the detailed processing flow focused on reflection-specific enhancements and amplitude analysis. A process referred to as "up-tuned, multi-path processing" was used on these data sets. Instrumental to this type of processing was the modification of the basic processing flow with each step, cycling back to previous steps to improve parameters based on downstream analysis (Figure 20). Subsequent time-lapse data sets were incorporated into reprocessing of preceding data sets to ensure all data underwent identical processing flows. Signal-enhancement processing focused on noise removal and improvement of spectral richness (Figure 21). Data similarity between the various monitor surveys was excellent, with no need for equalization processing to produce comparable preliminary seismic volumes (Figure 22).

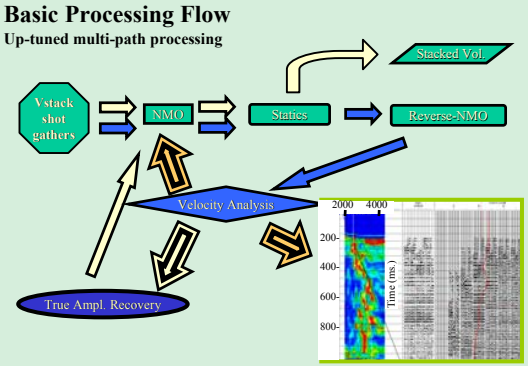

Figure 20. General processing flow.

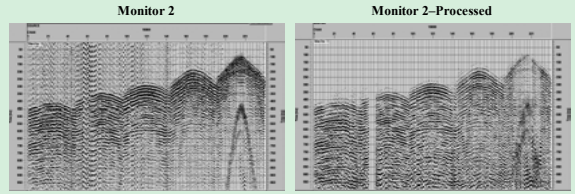

Figure 21. Signal enhancement comparison.

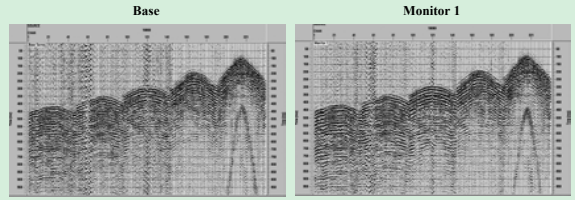

Figure 22. Similarity of different surveys.

Resolution

- Vertical (temporal) resolution: $h > \frac{1}{4}\lambda$
- Horizontal (spatial) resolution: $r \approx \sqrt{\frac{1}{2}\lambda D}$
  - Fresnel zone radius: $r \approx \frac{1}{2} V \sqrt{T_0/f}$

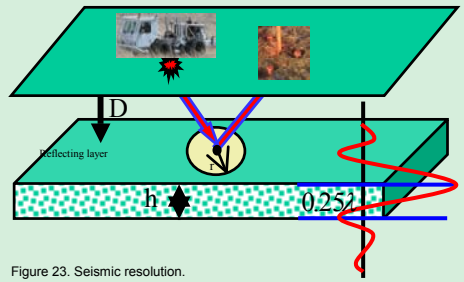

Figure 23. Seismic resolution.

Key to the effectiveness of seismic-reflection imaging in many medium and small midcontinent carbonate reservoirs is resolution, in particular vertical resolution, or the thinnest bed that can be distinguished from a seismic wavelet (Figure 23). It is generally assumed that one-quarter of a wavelength is the thinnest a bed can be and still detect top and bottom of the bed. These CMP stacked data possess a dominant frequency of around 90 Hz with a usable upper-corner frequency of about 180 Hz at the depth of interest. These data characteristics equate to a bed-resolution potential of around 7 m at 900 m below ground surface. With enhancement processing the dominant frequency is expected to improve to around 120 Hz to 140 Hz allowing a bed-resolution potential of around 4 m.

Considering the importance of spatial tracking of the CO_2 plume as it moves across this site, horizontal resolution is a key to how effective high-resolution seismic can be monitoring any EOR program. It is commonly accepted that a fraction of the radius of the first Fresnel is approximately equivalent to the size an object must be to distinguish it as unique on a seismic section. The Fresnel radius for data from this study is about 100 m at 900 m below ground surface (Figure 24). Therefore, any object 100 m or larger can be uniquely detected with these seismic data. However, changes in seismic-data character (possibly indicative of changes in fluid) significantly smaller than the radius of the Fresnel zone can be detected.

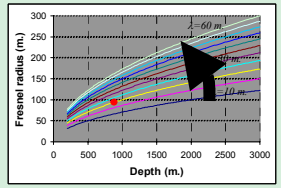

Figure 24. Horizontal resolution at site.

CMP Stacked Section: Seismic Cube

In general, the data quality across this site is quite good at the L-KC depth of around 550 ms (Figure 25). The various seismic cubes can be sliced inline or crossline relative to the receiver lines to produce 2D cross sections. Coherent reflections are prevalent within the time window of interest (300 ms to 700 ms).

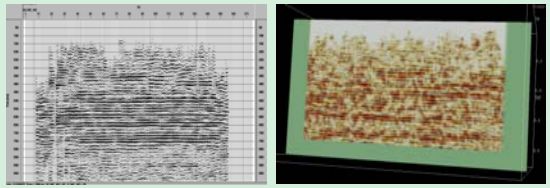
Figure 25. 2D inline time slice of seismic cube.

Interpretations of time slices tend to support both structural and stratigraphic influences on accumulation and movement of fluids through the L-KC horizon (Figure 26). Some sense of the lithologic trends potentially influencing well performance can be gained by comparing and contrasting apparent boundaries or lineaments and changes in texture of specific seismic properties across the site.

A prominent feature evident in both data sets is a contrast in properties north and south of an east/west-trending line (A) lying immediately south of well #18 (Figure 26b&d). This trend (A) marks a substantial change in seismic character (both amplitude and frequency) and may indicate the presence of a structural feature or an abrupt change in rock properties. Another lineament (B) follows an amplitude high (red) trend (Figure 26b) and an anomalous group of frequency cells (Figure 26d). This feature, though subtle on both data sets, exhibits a sufficiently high contrast to indicate a marked change in rock properties. A third more subtle northeast/southwest-trending lineament (C) marks a texture change in frequency and an apparent alignment of anomalies in amplitude. Because of the greater sensitivity instantaneous frequency has to lateral lithologic changes compared to instantaneous amplitude, it seems likely this lineament (C) is related to lithology. It is unlikely this lineament (C) would have been interpreted from amplitude plots alone.

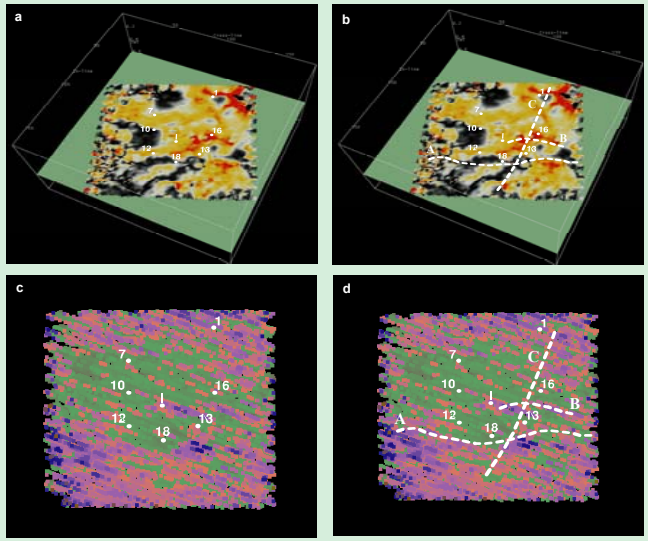

Figure 26. Both amplitude (a) and frequency attribute plots (c) representing an over 30-m-thick interval of rock that includes the subsurface interval of interest plus around 20 m of rock overlying and underlying C zone at this site possess structural and stratigraphic features (b and d) consistent with known lithology, but at much greater resolution.

Time-to-Depth Correlations

A vertical seismic profile (VSP) was acquired in well #16 and, when correlated with well logs, provided an excellent basis for time-to-depth conversions. Data were acquired with a 24-channel hydrophone stringer (Figure 27A). Seismic arrivals trailing the first arrivals were contaminated with tube wave, which hampered full VSP analysis Figure 27B). Using the time-to-depth conversion, it is possible to bulk time-correct the synthetic seismogram for the normal inaccuracy (< 10%) in absolute time resulting from estimating overburden velocity.

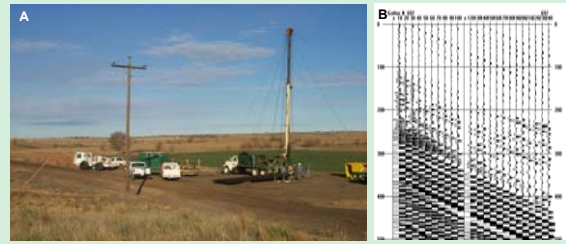

Figure 27. VSP survey at well #16 (A), seismogram from borehole (B).

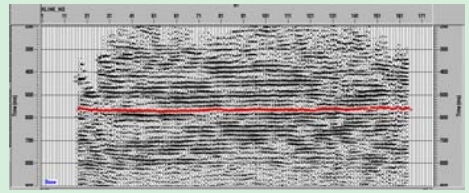
Figure 29. "C" zone horizon on 2D time slice.

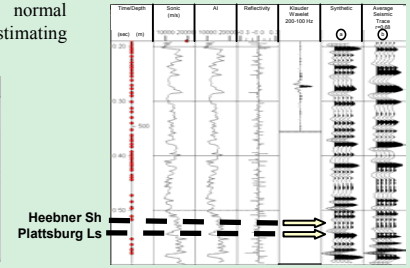

Figure 28. Synthetic compared to real.

Sonic logs from the CO_2 injection well and well #16, combined with a seismic wavelet extracted from real data, were used to generate a conventional synthetic seismogram (Figure 28). A C zone horizon time of 548 ms, established by incorporating the VSP and manual wavelet-correlation techniques, was tracked across all the 3D-seismic volumes (Figure 29). Considering CO_2 injection interval is only 5 m thick—equating to little more than 1 ms—it was imperative to accurately identify the L-KC "C" reflection within a few tenths of a percent.

Seismic Modeling and Fluid Replacement

Gassmann's relations can be used to estimate rock-bulk modulus change for the two (effective fluid) pore-fluid compositions. For our case the two-fluid composition includes the combination of oil-water and miscible CO_2-oil-water. Average composition effects of reservoir pore-fluid replacement on rock property suggests the maximum imageable changes will occur once saturation levels reach 0.28, at which point a difference of about 10% in seismic amplitude should be expected (Figure 30).

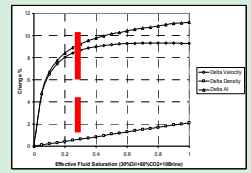

Figure 30. Fluid replacement model.

Attribute Analysis

Lithologic relationships or trends should be observable on lineament-attribute maps of the horizon interpreted as the L-KC "C" (Figure 31). A strong northeast/southwest series of lineaments are evident across the entire horizon. The most pronounced of these lineaments lies between CO_2I#1 and well #13 and extends across the entire survey area (Figure 32). Another notable lineament extends from about well #13 west between well #12 and injector #18 (Figure 32). Also evident is a secondary trend of much smaller and more discontinuous lineaments with a more east-northeast/west-southwest trend, especially pronounced in the northern half of the survey area.

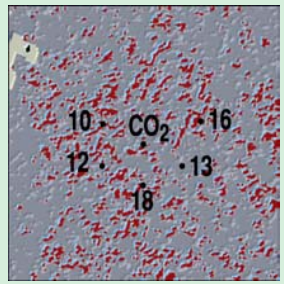

Figure 31. Lineament map "C" horizon.

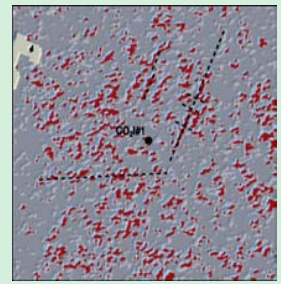

Figure 32. Interpreted lineament map.

A similarity-facies-attribute map overlain by the L-KC horizon time-structure map provides possible lithologic explanations for the rate and path of CO_2 movement (Figure 33). A northeast/southwest lithologic trend is evident on the facies map. After careful study, it is clear the reservoir near well #13 appears both topographically and lithologically different relative to rocks around wells #12 and CO_2I#1. This difference is likely associated with the observed and somewhat unexpected response at well #13. Interpretations of these attributes in conjunction with production data support the suggestion of a complex shoal depositional motif, consistent with the fact oolitic lithofacies are the known reservoir in this interval. (See discussion below and Figures 35 and 36.)

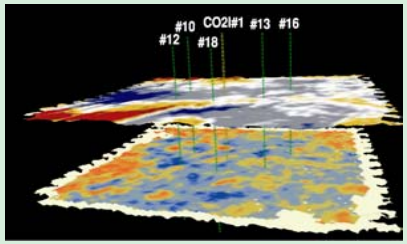

Figure 33. Time structure over similarity facies of "C" horizon.

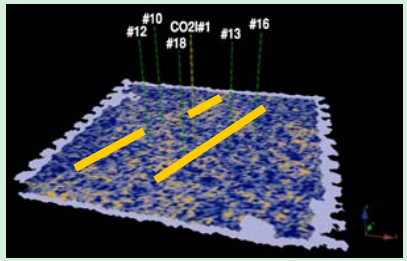

Figure 34. Lineament of "C" horizon.

Carbonate Facies and Architecture Control

The vertical and lateral heterogeneity in reservoir properties (permeability/pressure barriers or sealing discontinuities) has been suggested as an explanation for the differences between observed and predicted post-CO_2-production data. A seismic-lineament map (Figure 34) provides a possible explanation for the discrepancy between observed/measured time-lapse monitoring and production data and predicted reservoir-simulation movement of the EOR-CO_2 bank. Interpreted seismic lineaments NNE-SSW on the similarity-seismic facies (Figure 33) and lineament-attribute maps (Figure 34) play an important role in providing an image of the interconnectivity between the better reservoir-quality rocks.

The depositional environment for the "C" zone in the Hall-Gurney field area is interpreted as a tidally dominated ooid shoal complex, which other studies have shown to be a common depositional motif for similar cyclothemic strata throughout the Pennsylvanian in Kansas. Relatively few published land-based 3D-seismic surveys have focused on oolitic reservoir systems. Those that have been published are at the typical industry resolution and result only in larger-scale delineation of general shapes on the order of tens of meters. The data in our study allow resolution of the Hall-Gurney oolite shoal complex in the "C" zone at a scale of approximately 5 m.

Studies in the Modern and Ancient show that ooid shoal depositional environments are complex in regard to lithofacies distribution. Although seismic-similarity facies maps in our study are averaged over a thickness of approximately 5 m and reflect several stacked oolitic deposits, they are providing a level of detail that can be more closely related to features observed within individual oolitic shoal complexes (Figures 35 and 36).

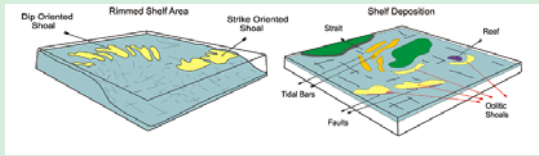

Figure 35. Cartoons showing settings where ooid shoals commonly develop and typical geometries of ooid bodies, including linear, pod-shaped, curved, and parabolic forms. Note structure (e.g., faults) can exert a control on ooid shoal development, which may be an important element in controlling depositional patterns in the Hall-Gurney field.

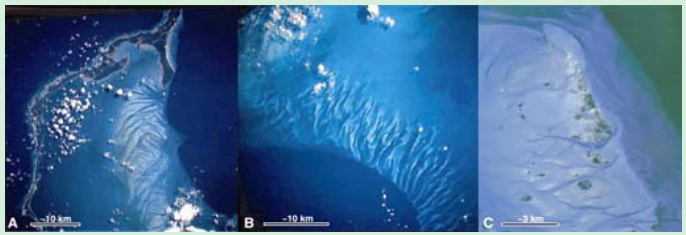

Figure 36. Modern oolite shoal examples. A) Southern part of Eleuthera Island in the northern Bahamas. Dark blue is deep water and light blue is shallow-water platform area. Oolite shoals (lightest color) near the edge of platform are curved, elongate bodies that are dissected by tidal channels. NASA Photo ID: STS066-88-056. B) A portion of the Tongue of the Ocean (dark blue, bottom left) and the Bahamas Bank (light blue). Oolite shoals near the edge of the bank are elongate and parabolic in shape. NASA Photo ID: STS005-37-839. C) Joulter's Cay area of the Bahamas showing ooid shoal complex (light-gray areas) dissected by tidal channels. Note pod shapes of some bodies.

In looking at the similarity patterns on Figure 33, it is not unreasonable to interpret sinuous to linear, isolated pod-shaped, and apparent parabolic features on the similarity map as reflecting small-scale depositional features within an ooid shoal depositional system, with blue areas representing ooid-dominated shoals (good reservoir quality) and golden to red areas representing inter-shoal depositional environments and differing lithofacies characterized by poorer reservoir quality.

In addition to depositional lithofacies patterns, it is apparent that structural elements, including lineaments, contribute to heterogeneity in Hall-Gurney field and may have influenced the location of depositional lithofacies, including location of ooid sand bodies (Figures 34 and 35).

4D-Seismic Monitoring Flood

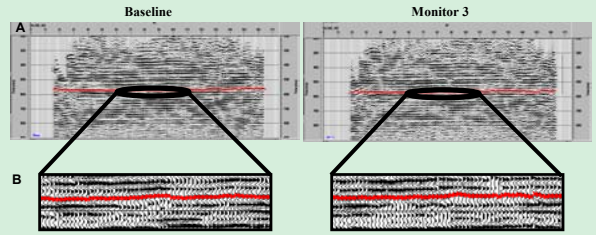

Figure 37. Differences in seismic data between surveys.

A baseline and five 3D surveys have been acquired and preliminary processed with first-pass interpretations completed on four 3D data volumes. Reflections identified on synthetic seismic traces and VSP as the top of the "C," and consistent with core and log data, were traced throughout the seismic volume (Figure 37A). Even though subtle changes at and below the reservoir horizon at locations consistent with CO_2 injection models are evident on 2D cross sections (Figure 37B), correlating seismic observations with physical changes expected and/or possible in reservoir rocks requires the greater sensitivity of attribute analysis.

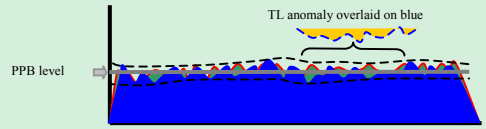

Figure 38. Parallel progressive blanking technique.

Considering the expected need to image a seismically weak change in properties (very near background noise levels) as a result of EOR-CO_2 fluid replacement, we developed and applied an approach that avoids differencing monitor data with baseline data (Figure 38). Our approach uses parallel progressive blanking (PPB), color balancing, and color focusing of each data set independently. Using this approach to interpretation, no differencing is necessary and therefore we avoid global equalization routines that make the assumption that changes between surveys can be compensated for by balancing based on user-defined background areas.

Amplitude Envelope

After the horizon interpreted as the L-KC "C" was identified on all 3D seismic cubes (baseline and first five monitor surveys), the amplitude envelope attribute was calculated for the L-KC horizon (Figure 39). Amplitude envelope, or reflection strength, seismic attribute was selected because of its insensitivity to small phase shifts. This is especially important for this data set because the vibrator used for this study was not phase locked; minor variations in wavelet phase should be expected from survey to survey and shot to shot. Seismic-reflection data for this study are all recorded uncorrelated, providing the opportunity during the later years of this study to apply phase-compensation filters prior to correlation.

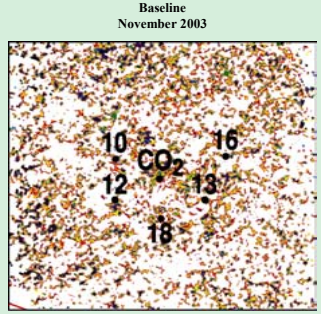

Figure 39. Amplitude envelope of horizon.

Average-amplitude envelope is phase and frequency independent, more stable in terms of susceptibility to noise contamination, when compared to many other seismic attributes, and has proven to be one of the most robust and tolerant to inconsistencies associated with phase fluctuations. This attribute provides higher tolerance to imperfections due to cross-equalization practices. Those properties, besides being instantaneous, make average "median" amplitude-envelope attribute an excellent candidate for time-lapse studies. For our application we used a "median value" of five samples around the time horizon.

4D-Seismic Interpretation

Currently, preliminary processing and interpretation have been completed on the baseline and first three monitor surveys. Amplitude-envelope attribute data for these surveys possess changes in texture generally consistent with expectations and CO_2 volumetrics (Figure 40). Arguably, there are a multitude of different boundaries that could be drawn to define the shape of the CO_2 plume, but the shapes suggested match the physical restraints, based on engineering data and the estimated amplitude response. Focusing on the injection well area and continuity of the characteristics defining the anomalous area, it is not difficult to identify a notable change in data character and texture likely associated with the displacement of reservoir fluids with CO_2.

Advancement of the CO_2 from the injector seems to honor both the lineaments identified on baseline data and changes in containment pressures. Overlaying the amplitude-envelope attribute map with the lineament attribute map provides an enhanced view, and therefore perspective, of the overwhelming variability in the reservoir rocks and the associated consistency and control these features or irregularities have on fluid movement (Figure 41).

Increased northerly movement of the CO_2, as interpreted on seismic data and inferred from production data, after several months of CO_2 injection and oil production, stimulated an increase in injection rates at the water-flood wells (Figure 41B). After several months of increased water-injection rates, the CO_2 advancement to the northwest was halted and some regression was observed on seismic data (Figure 41A). Production data did not refute the suggested receding of the CO_2 front near injection well #10; however, insufficient well coverage exists to provide monitoring at the seismic-resolution levels.

Interpretations of time-lapse seismic data are consistent with and can assist understanding actual field response data for this pilot study. In a similar fashion, 4D seismic could clearly provide essential input to reservoir simulations necessary for full field EOR-CO_2 floods. Key observation from seismic data include:

- accurate indication of solvent "CO_2" breakthrough in well #12,
- predicted delayed response in well #13,
- the interpretation of a permeability barrier between wells #13 and CO_2I#1, and
- consistency with reservoir-simulation prediction of CO_2 movement and volume estimated to have moved north, outside the pattern.

Seismic Results to Enhance Reservoir Simulations

Simulators are only as "good" as the quality and resolution of the reservoir properties and characteristics that make up the models. Initial simulator runs incorporated models based on pre-injection production and well data alone. These predictions were very dissimilar to actual production measured after commencing EOR-CO_2 injection. All interpretations of seismic data were accomplished without the aid of simulations updated with the most current production data; therefore, to a limited extent, the interpretations of CO_2 movement on seismic data were accomplished somewhat "blind." Predictions of breakthrough at #12 and the delay at #13 were based on seismic data alone after the second monitor survey. General changes in the CO_2 plume and resulting measurements at production wells have been consistent throughout the flood.

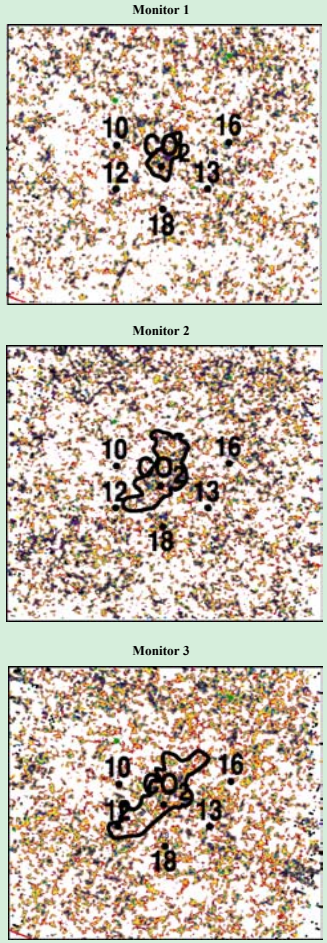

Figure 40. Comparison of amplitude horizon.

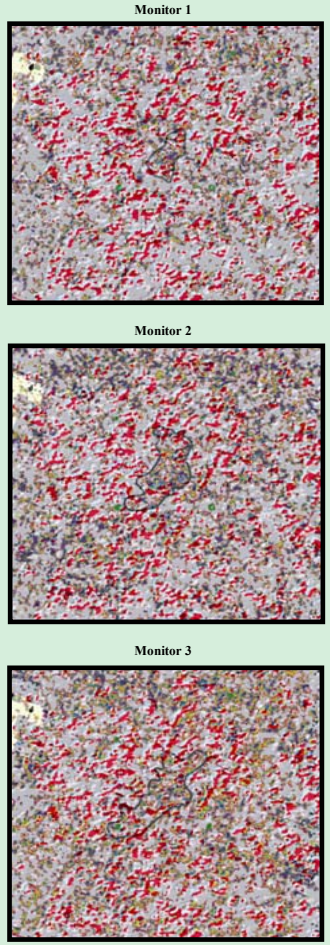

Figure 41. Comparison of amplitude envelope over lineaments.

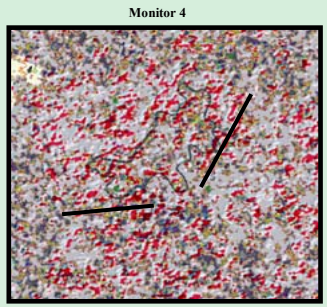

Figure 42. Interpretation of CO_2 and geologic controls.

Interpretations of geologic features from seismic data have provided critical location-specific reservoir properties that appear to strongly influence fluid movement in this production interval. Lineaments identified on seismic sections likely (based on time-lapse monitoring and production data) play a role in sealing and/or diverting flow through the reservoir (Figure 42). By incorporating these features using properties consistent with core data, a more realistic reservoir simulator results, honoring the production and core properties (Figure 43). Flow models after simulator updating (sealing lineaments and preferential permeability manifested by faster progression of the CO_2 bank) show great improvement in detail and provide excellent correlation with the material balance (Figure 44).

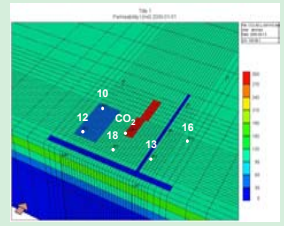

Figure 43. Variability of permeability based on production and seismic.

Conclusions

Time-lapse seismic monitoring of EOR-CO_2 can reveal weak anomalies in thin carbonates below temporal resolution and can be successful with moderate cross-equalization and attention to consistency in acquisition and processing details. Most of all, methods applied here avoid the complications associated with inversion-based attributes and extensive cross-equalization techniques.

Shortness of turnaround time of time-lapse seismic monitoring in the Hall-Gurney field provided timely support for reservoir-simulation adjustments and flood-management requirements across this very short-lived pilot study.

Spatial textural, rather than spatially sustainable magnitude, time-lapse anomalies were observed and should be expected for thin, shallow carbonate reservoirs. Non-inversion, direct seismic attributes proved both accurate and robust for monitoring the development of this EOR-CO_2 flood.

Distribution and geometries associated with similarity-seismic facies and seismic-lineament patterns are suggestive of a complex ooid shoal depositional motif, consistent with oolitic lithofacies being the known reservoir in this field. Oolitic facies are imaged on these seismic data at a resolution significantly greater than previously documented.

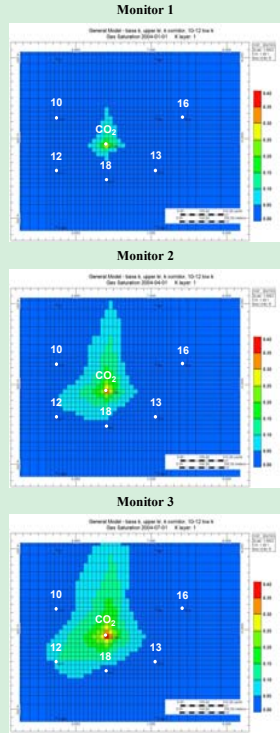

Figure 44. Simulations for seismic survey times.

Acknowledgments

Support for this project was provided by the National Energy Technology Laboratory at the U.S. Department of Energy under grant DE-FC26-03NT15414.